Molecular Dynamics Simulation of the Adsorption of Mung Bean Defensin VrD1 to a Phospholipid Bilayer

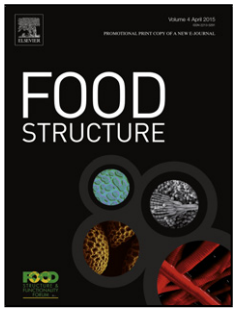

Title: Molecular Dynamics Simulation of the Adsorption of Mung Bean Defensin VrD1 to a Phospholipid Bilayer

Authors: Huda A. Alghamdi, Lydia J. Campbell, Stephen R. Euston

PII: S2213-3291(19)30013-9
DOI: https://doi.org/10.1016/j.foostr.2019.100117
Article Number: 100117

Reference: FOOSTR 100117

To appear in:

Received date: 4 February 2019
Revised date: 23 April 2019
Accepted date: 16 May 2019

Please cite this article as: Alghamdi HA, Campbell LJ, Euston SR, Molecular Dynamics Simulation of the Adsorption of Mung Bean Defensin VrD1 to a Phospholipid Bilayer, *Food Structure* (2019), https://doi.org/10.1016/j.foostr.2019.100117

Molecular Dynamics Simulation of the Adsorption of Mung Bean Defensin VrD1 to a Phospholipid Bilayer

Huda A. Alghamdi[1], Lydia J. Campbell[2] & Stephen R. Euston[2]*

[1]Department of Biology, College of Science, King Khalid University, Abha, Saudi Arabia

[2]Institute of Mechanical, Process and Energy Engineering, Heriot-Watt University, Edinburgh, EH144AS, UK

***Corresponding author: S.R.Euston@hw.ac.uk**

Graphical abstract

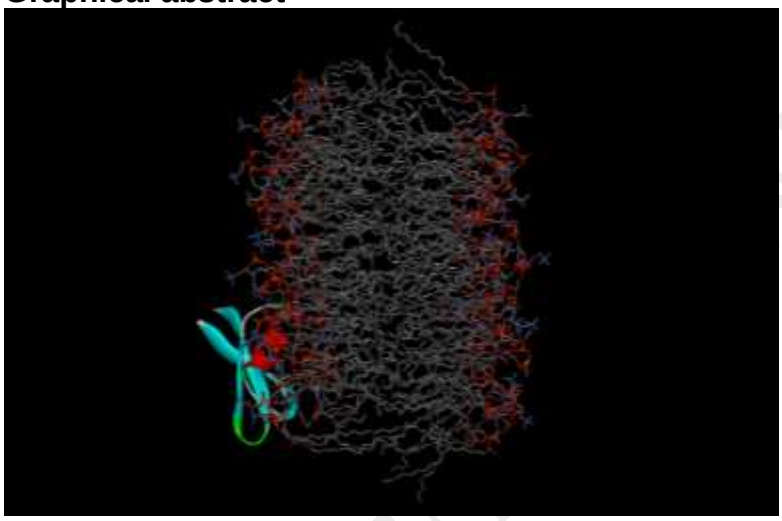

Highlights

- Adsorption of defensin VrD1 to a DPPC bilayer is mediated by electrostatic interactions
- Cationic lysine and arginine residues interact with anionic DPPC head groups
- Penetration of VrD1 into bilayer decreases acyl chain order and disrupts bilayer structure

Abstract

Defensins are small peptides with anti-microbial properties and potential use as anti-fungal agents in foods. Molecular dynamics simulation elucidated the mechanisms of anti-fungal activity, by following the interaction between mung bean defensin VrD1 peptide and a diphosphatidylcholine (DPPC) bilayer. VrD1 interacts with the bilayer,

initially, via electrostatic interaction between cationic amino acid side chains of lysine and arginine and the negatively charged DPPC head group. This initial docking of the VrD1 with the interface is independent of the peptide orientation at first approach, and is similar to the mechanism observed for lysozyme, also a cationic protein. Gradual penetration of the VrD1 peptide into the acyl chain leaflet of the bilayer follows. Some change to the tertiary fold of the protein occurs upon insertion of the peptide into the bilayer, but no significant changes to the secondary structure, with evidence of a stabilization of the VrD1 conformation upon adsorption. The net effect of VrD1 penetration into the bilayer is a disruption of the acyl chain order in the DPPC, which in a cell membrane would lead to disruption of metabolic processes and ultimately to cell death.

Keywords: protein adsorption; defensin; molecular dynamics; phospholipid bilayer; anti-fungal

Introduction

Defensins are a group of small globular peptides that have antimicrobial activity and contribute to the innate immune response of plants and animals (Cumac et al., 2019). This has led to interest in them as antifungal agents in foods. Their structure is highly conserved across species, with, typically, 45-54 amino acids, and a conserved secondary structure comprised of three antiparallel β-sheets and an α-helix (Liu et al., 2006). Four strictly conserved disulphide bridges hold the structure together (Liu et al., 2006).

Details of the mechanism by which defensins kill fungal cells remain unclear, although there are several hypotheses to explain this. The most favoured hypothesis

proposes cationic amino acid side chains of the defensin to associate with negatively charged regions of the cell membrane through electrostatic interactions (Yeamn & Yount, 2003). The bound peptides penetrate the membrane and form pores, causing cell death by allowing ions and metabolites to leak from the cell. Three distinct models are proposed to explain pore formation mechanisms for plant defensins - the barrel-stave, toroid pore (or wormhole) and carpet mechanisms (Pelegrini, del Sarto, Silva, Franco & Grossi-de-Sa, 2011). In two of these mechanisms (barrel-stave and toroidal pore) a barrel shaped pore is believed to form, although the details differ between the two. The barrel-stave mechanism involves insertion of a hydrophobic region of the defensin into the membrane, which is stabilised by interaction with the acyl chains of the phospholipid. As more defensins enter the membrane, the protein reaches a critical concentration of protein where they self-associate and form a barrel ring structure opening a pore in the membrane. In this, hydrophobic regions of the defensin structure are on the outside of the barrel, with the inside of the pore lined by hydrophilic regions of the peptide. In the toroidal pore mechanism, proteins and phospholipid head groups overlap leading to a curvature of the membrane and eventual rupture. In the final mechanism no discrete pores form. Rather, a monolayer (carpet) of defensins forms via electrostatic interactions, causing displacement of membrane phospholipids, and changes to membrane fluidity, which eventually leads to membrane disruption followed by cell death.

In this study, all atom molecular dynamics (MD) simulation probes the interaction of mung bean defensin VrD1 with a dipalmitoyl phophatidylcholine (DPPC) bilayer. VrD1 (Figure 1) has the conserved defensin secondary structure (α-helix, and a three stranded β1, β2 and β3 anti-parallel β-sheet) and a short 3_{10} helix. Two disulphide bonds (Cys19-Cys40 and Cys23-Cys42) bridge the α-helix and β3 strand.

A further disulphide bond (Cys13-Cys33) connects the β2 strand and loop 1 (which joins the α- and 3_{10} helices), and a final disulfide bond (Cys3-Cys46) ensures a compact close packed globular tertiary structure by linking the N and C terminal ends. There is a further random coil loop (loop 2) between the β2 and β3 strands. Defensins contain around 17% of charged amino acids. Of these, arginine and lysine, both cationic amino acids account for over 70% of the charged amino acids (Wang & Wang, 2004). Through simulation of the adsorption of the VrD1 molecule to the DPPC bilayer, we will obtain information that will help to determine the mode of interaction with cell membranes and the mechanism by which defensins elicit cell death.

Molecular dynamics simulation complements experimental studies as it gives atomic scale detail of adsorbed protein conformation (Euston, 2014; Dalkas & Euston, 2019). MD simulations of protein adsorption at air-water and oil-water interfaces have included barley lipid transfer protein (LTP), a peptide important in the formation and stabilization of beer foam (Euston, Hughes, Naser & Westacott, 2008a; 2008b; Euston, 2010) and hydrophobins (Euston, 2014), fungal surfactant proteins with exceptional foaming ability and potential as foaming and emulsifying agents in foods.

Simulation Methodology

Simulations were carried out using the molecular dynamics package GROMACS (version 4.05) (Hess, Kutzner, van der Spoel & Lindahl, 2008). The NMR structure determined by Liu et al (2006) of the VrD1 defensin isolated from mung bean was used in this study. A phospholipid bilayer-water interface was constructed to simulate the adsorption of the VrD1 at the bilayer interface. A method reported previously (Euston, 2014) was used to build a di-phosphatidyl-choline (DPPC) bilayer interface

using a pre-equilibrated DPPC billayer deposited on the GROMACS websites (www.gromacs.org) by Chiu et al. (2009). This comprised one hundred DPPC molecules, arranged in two leaflets with fifty DPPC in each leaflet. A vacuum space was formed on each side of the bilayer by expanding the box in the z- coordinate dimension, and a single defensin molecule inserted on one side of the bilayer, followed by addition of SPC water (Berweger, van Gunsteren & Muller-Plathe, 1995) to a density of 1000 g/L. Energy minimization of the bilayer-water-defensin system was by a conjugate gradients algorithm (Hestenes & Stiefel, 1952). For the main simulation run, coulomb interactions (cut-off of 1.0 nm), and Van der Waals interactions (cut-off of 1.6 nm) were summed using the particle mesh Ewald (PME) method (Darden, York, & Pedersen, 1993; Essmann et al., 1995) with force-field parameters defined by the modified GROMOS 43a2-S3 force field (Chiu, Pandit, Scott & Jakobsson, 2009).

Production simulation runs were carried out in the isothermal-isobaric (NpT) ensemble for a time period of up to 360ns with temperature controlled using the Nose-Hoover thermostat (Nose, 1984; Hoover, 1985) set to 300K. A Parrinello-Rhaman barostat (Parrinello, & Rahman, 1981; Nose & Klein, 1984) was used to control pressure to 1 bar with semi-isotropic pressure coupling allowing the pressure in the x-y plane to be controlled independently of the pressure in the z-direction normal to interface.

Trajectories were analysed using GROMACS tools to determine structural properties of the defensin molecule and DPPC bilayer. Determined parameters were the root mean square deviation (RMSD) of backbone atom positions relative to the starting native conformation; radius of gyration (R_g) of backbone atoms; secondary structure

changes (helices, sheets, and turns) using DSSP (Kabsch & Sander, 1983); the eccentricity (e, deviation from a perfect sphere) of the protein from the moments of inertia along the principle axes and the order parameter of the acyl chains of the DPPC molecules in the bilayer. The eccentricity, e, is given by the equation,

$$e = 1 - \frac{I_{min}}{I_{ave}} \qquad (1)$$

I_{min} is the smallest of the three moments of inertia, and I_{ave} the average of the three. The eccentricity takes the value e = 0 for a perfect sphere, and e approaches 1 for a rod.

Equation (2) defines the deuterium order parameter:

$$S_{CD} = \frac{1}{2}(3cos^2\langle\theta\rangle) \qquad (2)$$

where θ is the angle between the bond and the bilayer normal. S_{CD} = 1 means perfect alignment with the bilayer normal, S_{CD} = −0.5 anti-alignment, and S_{CD} = 0 random orientation. The interactions between the protein and DPPC were determined by calculating the total, van der Waals and electrostatic energy between protein and DPPC, and the conformational entropy (S). The conformational entropy of the protein and DPPC bilayer were estimated using the Boltzmann entropy equation,

$$S = -k_B \sum_i p_i \ln p_i \qquad (3)$$

where k_B is the Boltzmann constant and p_i the probability of a particular conformation of the protein or DPPC bilayer occurring. For this study, the root mean square deviation was used as a conformational marker. Clearly, this is an approximate method of defining unique conformations, but is accurate enough for an estimate of

entropy changes in this case. As a separate check of entropy changes for the protein alone, the conformational entropy for the VrD1 was calculated from the eigen vectors of the covariance matrix using Schlitters equation (Schlitter, 1993). This method is unsuitable for use with the DPPC bilayer.

Two different orientations of the protein adsorbed at the interface were simulated. These are labelled orientation 1 and orientation 2.

Results & Discussion

Figures 2 and 3 show snapshot conformations of VrD1 adsorbed to the DPPC bilayer-water interface. In orientation 1, the VrD1 molecule adsorbs initially, within about 1ns of the start of the simulation, via electrostatic interaction between a lysine residue (LYS34) in the loop 2 region (Figure 2b). This residue remains close to the surface, presumably anchoring the VrD1 to the bilayer, whilst a second lysine residue (LYS12 in loop1) recruits to the interface (Figure 2c). Over the next 5 ns the VrD1 molecule rolls onto the surface, maintaining contact between loop 2 and LYS34 and the DPPC layer, but rotating LYS12 and loop 1 away from the surface (Figure 2d-e). At the same time, this brings an arginine (ARG1) residue at the N-terminal end into contact with the surface. The electrostatic interaction with the LYS34 and ARG1 stabilizes the VrD1 conformation at the surface, which does not change significantly even as the protein inserts itself further into the DPPC bilayer. Consolidation of the adsorption of VrD1 occurs as loop 2 pushes further into the bilayer (Figure 2f-g), followed by the β-strands (Figure 2h-i), with the α-helix remaining outside the bilayer leaflet. Even though VrD1 in orientation 2 adsorbs to the DPPC bilayer through interactions with different amino acid residues, the mechanism of adsorption seems remarkably similar to that for orientation 1 (Figure 3). For orientation 2 initial contact

and anchoring to the bilayer is also through a positively charged amino acid (ARG26) at the C-terminal end of the α-helix (Figure 3b-c). After 6ns the molecule has rotated to bring a second positively charged residue (LYS7 at the end of the β1-sheet) in contact with the DPPC bilayer (Figure 3d-e). After 20ns (Figure 3f), the VrD1 molecule has rotated further to recruit ARG38 to interact with the DPPC layer. These three positively charged amino acid residues anchor the VrD1 in an orientation at the DPPC-water interface that changes little on further simulation, other than penetration of the protein into the leaflet of the bilayer (Figures 3g-i). The general sequence of events for the adsorption of the VrD1 in orientation 2 are the same as for orientation 1, although the timings differ, as does the final adsorbed conformation. Clearly, charged amino acids play a role in the interaction of VrD1 with the interface in both orientations. Of the ten positively charged amino acids, six in orientation 1 and five in orientation 2 adsorb to the bilayer-water interface in the final adsorbed conformation. This sequence of adsorption events is consistent with the theories for defensin interaction with membranes (Yeamn & Yount, 2003).

Simulations of various proteins have identified that some adsorb in a particular orientation at interfaces whilst others show no preference. Zare et al (2015, 2016) simulated the adsorption of the bovine whey protein β-lactoglobulin at a decane-water interface. In all cases the orientation in which the molecule adsorbed, and the amino acids interacting with the surface were very similar, even though several starting orientations of the protein were simulated. They also observed the importance of two lysine residues, with these making the initial contact with the interface in virtually all simulations. After initial adsorption, two regions rich in hydrophobic residues have a high likelihood to adsorb to the interface. Cheung (2017) simulated two proteins, lysozyme and α-lactalbumin, with contrasting

behaviour. Whilst α-lactalbumin tends to adsorb in a defined orientation controlled by two amphipathic helices, lysozyme adsorption is non-specific. Surfactant proteins such as hydophobins also have a preferred adsorption orientation (Euston, 2014), although the orientation differs depending on the interface type. Hydrophobins have a patch of hydrophobic amino acids on one face of the molecule. The hydrophobin adsorbs with this patch in contact with and parallel to the air-water and decane-water interface, but perpendicular to the more polar DPPC bilayer-water interface (Euston, 2014). The VrD1 defensin has adsorption behaviour more like lysozyme, i.e. it is non-specific. Interestingly, lysozyme like VrD1 is also a cationic protein, and this may suggest a shared adsorption mechanism mediated by electrostatic interactions for such molecules.

The amino acids that are adsorbed to the interface and embedded into the bilayer for both orientations of the VrD1 molecule are listed in Table 1, with the minimum distance of each residue (averaged over the final 40ns of the simulation) to the DPPC layer shown in Figure 4. For orientation 1, amino acid sequences at both the N- and C-terminal end adsorb. It is also noticeable that in orientation 1, eight of the ten hydrophobic amino acids in VrD1 are also adsorbed (Table 1), so clearly hydrophobic amino acid interactions with the surface also play a role. Several regions of the VrD1 primary sequence adsorb to the bilayer in both conformations, including a section from residues 6-18 (Figure 4).

Figure 5 shows the van der Waals and electrostatic (Coulombic) contributions to the interaction between the protein and the DPPC bilayer. For both interfaces, electrostatic interactions dominate over van der Waals forces, with both becoming increasingly negative over time, supporting the view that interaction between

positively charged amino acids and negatively charged DPPC head groups controls protein-surface interactions. For both conformations the van der Waals and electrostatic energy is similar up to approximately 100ns after which the interaction energies for orientation 1 become increasingly lower than for orientation 2. This reflects the greater number of amino acids (29 vs 17 for orientation 2) and charged side chains (6 vs 5) embedded in the DPPC bilayer for orientation 1 at the end of the simulation. It is noticeable that the van der Waals interactions seem still to be decreasing at the end of the simulation. This is likely to be because the defensin molecule is still penetrating into the bilayer structure, and we might realistically expect that this process occurs over longer than ns timescales. Not only a favourable change in the enthalpy of interaction, but also entropy changes to both the protein and the DPPC bilayer control the adsorption of the protein to the surface. The change in conformational entropy for a VrD1 molecule adsorbing to the DDPC layer is negative (-0.42k_B and -0.18 k_B from equation 2, and -200 J/mol.K and -140 J/mol.K from Schlitter's formula for orientation 1 and 2 respectively). How protein conformational entropy changes upon adsorption is unclear (Euston, 2004). Norde and Lyklema (1991) argue that protein conformational flexibility will decrease on adsorption, with the decrease in conformational entropy offset by an increase in entropy due to loss of secondary structure. To the contrary, there are proteins that display increased conformational flexibility at oil-water interfaces. Anderson et al. (2000) have used a Monte Carlo simulation to show that that adsorption of a lattice protein at an oil-water interfaces can lead to an increase in entropy as increased interfacial fluidity allows the protein chain to adopt a wider range of conformations than in the native state. In our simulations, the VrD1 conformational entropy decreases upon adsorption and penetration into the DPPC layer indicating that the

protein conformation is stabilised as amino acid residues penetrate the DPPC phase. In addition, there is no apparent loss of secondary structure. This is not unexpected, as it is likely that the membrane disrupting effect of the defensin requires that the secondary and tertiary structure be largely maintained. The defensin molecule in both orientations adsorb to the DPPC bilayer with little change in α–helix, β-sheet and other secondary structure elements throughout the course of the simulation (Figure 6). An increase in conformational entropy for the DPPC bilayer ($0.95k_B$ and $0.13\ k_B$ from equation 2) at least partially compensates the decrease in conformational entropy for the VrD1 defensin. It is not possible to say from these results whether the main driving force for adsorption is due to the entropy change in the DPPC layer or the enthalpy change due to electrostatic and van der Waals interactions, and both are likely to play a role in the adsorption mechanism.

Other measures of protein conformational change also point to low flexibility of the VrD1 adsorbed conformation. Figure 7 reveals that there is a little or no change in the RMSD of the backbone atoms of the defensin molecule in both orientations as it adsorbs to the bilayer surface. Similarly, the overall volume occupied by the protein does not change a great deal since the total radius of gyration (R_g in Figure 8) does not fluctuate significantly throughout the simulation for both orientations. The molecule does undergo some conformational rearrangement however, since the components of the radius of gyration in the x, y and z-axes change significantly during the course of the simulation (Figure 8). The x, y and z components R_g of defensin adsorbed in both orientations show a high degree of variability, much more so than the overall R_g. Figure 9 plots the eccentricity of the shape of the VrD1 molecule as a function of simulation time. In its native conformation, the VrD1 molecule is aspherical with an average eccentricity of 0.30 ± 0.03. In orientation 1

but not orientation 2 the eccentricity of the starting conformation is outside (and lower) than the range of average e values for the native conformation. This may suggest that being close to the DPPC surface is sufficient to perturb slightly the shape of the protein. Over time, both orientations of VrD1 show a small increase in eccentricity suggesting a slight elongation of the conformation when embedded in the DPPC layer. This suggests the protein is changing its shape at the interface, but with little overall change to the molecular volume.

As noted earlier, the entropy of the DPPC bilayer increases when the VrD1 molecule inserts into the outer leaflet. Changes in other parameters also indicate the effect of the defensin molecules on the structure of the DPPC bilayer. Further evidence for the disordering of the DPPC bilayer when VrD1 adsorbs comes from the order parameters of the bonds in the acyl chains of the DPPC bilayer. Figure 10 shows the order parameter for acyl chains of the DPPC bilayer when defensin adsorbs in orientation 1 or orientation 2 and for a DPPC bilayer with no adsorbed defensin. For the bilayers that contain adsorbed VrD1 the order parameter is plotted both for the bilayer leaflet containing the defensin, and the second leaflet from which the VrD1 is absent. The shape of the order parameter plots is typical of those observed for DPPC bilayers (Vermeer, De Groot, Réat, Milon & Czaplicki, 2007) and adopt values comparable to those we have observed previously with this model for the DPPC bilayer (Euston, 2014). The order parameter the acyl chains make to the normal of the interface decreases the further the bond is from the glycerol backbone as the chains become more disordered in the bilayer centre away from the water interface. The DPPC bilayer with no defensin is present shows the highest acyl chain order (Figure 10). When a VrD1 molecule adsorbs the acyl chains of the phospholipid leaflet into which it adsorbs become less ordered (decrease in S_{CD}, Figure 10) for

both orientations of the defensin. The disordering effect extends into the second leaflet even though the VrD1 does not extend into this region of the bilayer. Thus, interaction of VrD1 defensin with the DPPC leads to extensive disruption to the bilayer structure. VrD1 in orientation 1 has a slightly greater disordering effect than in orientation 2. Given the van der Waals and coulombic interactions are higher for orientation 1 during the later stages of the simulation (Figure 5), this indicates that the details of the interactions within the bilayer differ between the two orientations. We have seen the same disordering effect on a DPPC acyl chains when the fungal hydrophobin protein HFBI adsorbs to the bilayer (Euston, 2014). Like the VrD1 molecules, the HFBI molecule disorders the DPPC acyl chains in both leaflets of the bilayer, with the greater degree of disorder observed in the leaflet in which the protein adsorbs. The acyl chains in those DPPC directly below the embedded HFBI molecule show the greatest degree of disorder, with a still significant but lower loss of order seen in acyl chains adjacent to the protein molecule. Although, there are clearly similarities in the adsorption of the two proteins, HFBI differs from VrD1 in that it adsorbs to the interface via a hydrophobic patch, with electrostatic interactions between positively charged amino acids and the negatively charged DPPC not playing a dominant role.

Conclusions

Our molecular dynamics simulations have shown a clear link between the cationic amino acid side chains of lysine and arginine and the initial docking and subsequent consolidation of the adsorption of VrD1 defensin to the DPPC interface, in agreement with the current theories for defensin action (Yeamn & Yount, 2003). There is also a similarity to the way in which other cationic proteins such as

lysozyme adsorb to interfaces. Importantly for defensin biological activity, the initial adsorption consolidates through the penetration of the peptide into the DPPC bilayer membrane, leading to a disordering of the membrane that in cellular membranes ultimately would lead to disruption of cell metabolism. The current simulation results lend weight to theories of defensin action that involve electrostatic interaction with bilayers. However, it is not possible to determine the precise mechanism of pore formation from the current study. This will require larger scale simulations involving several defensin molecules in a larger membrane model.

Acknowledgments

HAA acknowledges receipt of a PhD Scholarship from the government of Saudi Arabia.

References

Berweger, C. D., van Gunsteren W. F., & Muller-Plathe, F. (1995). Force field parametrisation by weak coupling. Re-engineering SPC water. *Chemical Physics Letters*, *232*, 429-436. https://doi.org/10.1016/0009-2614(94)01391-8

Cheung, D. L. (2017). Adsorption and conformations of lysozyme and alpha-lactalbumin at a water-octane interface, *Journal of Chemical Physics*, *147*, 195101. https://doi.org/10.1063/1.4994561

Chiu, S-W, Pandit, S. A., Scott, H. L., & Jakobsson E. (2009). An improved united atom force field for simulation of mixed lipid bilayers. *Journal of Physical Chemistry B*, *113*, 2748–2763. https://doi.org/10.1021/jp807056c

Ciumac, D., Gong, H., Hu, X., & Lu, J. R. (2019). Membrane targeting cationic antimicrobial peptides. *Journal of Colloid and Interface Science*, *537*, 163-185. https://doi.org/10.1016/j.jcis.2018.10.103

Dalkas, G., & Euston, S. R., (2019). Molecular Simulation of Protein Adsorption and Conformation at Gas-Liquid, Liquid-Liquid and Solid-Liquid Interfaces. *Current Opinion in Colloid & Interface Science*, *41*, 1-10. https://doi.org/10.1016/j.cocis.2018.11.007

Darden, T. York, D., & Pedersen, L. (1993). Particle Mesh Ewald - an N.Log(N) method for Ewald sums in large systems. *Journal of Chemical Physics*, *98*, 10089–10092. https://doi.org/10.1063/1.464397

Essmann, U., Perera, L., Berkowitz, M. L., Darden, T., Lee. H., & Pedersen, L. (1995). A smooth particle mesh Ewald method. *Journal of Chemical Physics*, *103*, 8577– 8593. https://doi.org/10.1063/1.470117

Euston, S. R. (2004). Computer simulation of proteins: adsorption, gelation and self-association. *Current Opinion in Colloid & Interface Science*, *9(5)*, 321-327. https://doi.org/10.1016/j.cocis.2004.09.005

Euston S. R. (2010). Molecular dynamics simulation of protein adsorption at fluid interfaces: a comparison of all-atom and coarse-grained models. *Biomacromolecules*, *11*, 2781-2787. https://doi.org/10.1021/bm100857k

Euston, S. R. (2014). Molecular simulation of adsorption of hydrophobin HFBI to the air–water, DPPC–water and decane–water interfaces. *Food Hydrocolloids*, *42*, 66–74. https://doi.org/10.1016/j.foodhyd.2013.12.005

Euston, S. R., Hughes, P., Naser, M. A., Westacott, R. E. (2008a). Comparison of the adsorbed conformation of barley lipid transfer protein at the decane-water and vacuum-water interface: a molecular dynamics simulation. *Biomacromolecules*, *9*, 1443-53. https://doi.org/10.1021/bm701227g

Euston, S. R., Hughes, P., Naser, M. A., Westacott, R. E. (2008b). Molecular dynamics simulation of the cooperative adsorption of barley lipid transfer protein and cis-isocohumulone at the vacuum-water interface. *Biomacromolecules*, *9*, 3024-32. https://doi.org/10.1021/bm8004325

Hestenes, M. R. & Stiefel, E. J. (1952). Methods of conjugate gradients for solving linear systems. *Journal of Research of the National Bureau of Standards*, *49*, 411-436. http://dx.doi.org/10.6028/jres.049.044

Hoover, W. G. (1985). Canonical dynamics: Equilibrium phase-space distributions. *Physical Review A*, *31*, 1695–1697. https://doi.org/10.1103/PhysRevA.31.1695

Kabsch, W., & Sander, C. (1983). Dictionary of protein secondary structure: pattern recognition of hydrogen-bonded and geometrical features. *Biopolymers*, *22*, 2577-2637. https://doi.org/10.1002/bip.360221211

Liu, Y. J., Cheng, C. S., Liu, Y. N., Hsu, M. P., Chen, C. S., & Lyu, P. C. (2006). Solution structure of the plant defensin VrD1 from mung bean and its possible role in insecticidal activity against bruchids. *Proteins*, *63*, 777-786. https://doi.org/10.1002/prot.20962

Norde, W. and Lyklema, J. (1991). Why proteins prefer interfaces. *Journal of Biomaterials Science, Polymer Edition*, *2(3)*, 183-202. https://doi.org/10.1080/09205063.1991.9756659

Nose, S. (1984). A unified formulation of the constant temperature molecular-dynamics methods. *Journal of Chemical Physics*, *81*, 511–519. https://doi.org/10.1063/1.447334

Nose, S. & Klein, M. L. (1983). Constant pressure molecular dynamics for molecular systems. *Molecular Physics*, *50*, 1055-1076. https://doi.org/10.1080/00268978300102851

Parrinello, M. & Rahman, A. (1981). Polymorphic transitions in single crystals: A new molecular dynamics method. *Journal of Applied Physics*, *52*, 7182-7190. https://doi.org/10.1063/1.328693

Pelegrini, P. B., del Sarto, R. P., Silva, O. N, Franco, O. L., Grossi-de-Sa, M. F. (2011). Antibacterial peptides from plants: what they are and how they probably work. *Biochemistry Research International*, *2011*, 1-10. https://doi.org/10.1155/2011/250349

Schlitter, J. (1993). Estimation of absolute and relative entropies of macromolecules using the covariance matrix. *Chemical Physics Letters*, *215(6)*, 617-621. https://doi.org/10.1016/0009-2614(93)89366-P

Vermeer, L. S., De Groot, B. L., Réat, V., Milon, A. and Czaplicki, J. (2007). Acyl chain order parameter profiles in phospholipid bilayers: computation from molecular

dynamics simulations and comparison with 2 H NMR experiments. *European Biophysics Journal*, *36(8)*, 919-931. https://doi.org/10.1007/s00249-007-0192-9

Wang, Z. & Wang, G. (2004). APD: the antimicrobial peptide database. *Nucleic Acids Research*, *32*, D590–D592. https://doi.org/10.1093/nar/gkh025

Yeamn M. R. & Yount, N. Y. (2003). Mechanisms of antimicrobial peptide action and resistance. *Pharmacology Reviews*, *55*, 27–55. https://doi.org/10.1124/pr.55.1.2

Zare, D., McGrath, K.M., Allison, J.R. (2015). Deciphering beta-lactoglobulin interactions at an oil-water interface: A molecular dynamics study. *Biomacromolecules*, *16*, 1855-61. https://doi.org/0.1021/acs.biomac.5b00467

Zare, D., McGrath, K.M., Allison, J.R. (2016). Molecular dynamics simulation of beta-lactoglobulin at different oil/water interfaces. *Biomacromolecules, 17*, 1572-81. https://doi.org/10.1021/acs.biomac.5b01709

Table Legends

Table 1 – Amino acid residues adsorbed to the DPPC-water interface for the two orientations of the adsorbed defensin molecule.

Adsorbed Amino-acids in orientation 1	Adsorbed Amino-acids in orientation 2
ARG1 (positively charged)	ILE5 (hydrophobic)
THR2	LYS6 (positively charged)
CYS3	LYS7 (positively charged)
MET4 (hydrophobic)	GLU8
ILE5 (hydrophobic)	GLY9
LYS6 (positively charged)	TRP10 (hydrophobic)
LYS7 (positively charged)	GLY11
LSY12 (positively charged)	LYS12 (positively charged)
CYS13	HIS21
LEU14 (hydrophobic)	SER22
ILE15 (hydrophobic)	CYS23
ASP16	LYS24 (positively charged)
THR17	ASN25
THR18	ARG26 (positively charged)
CYS19	GLY27
ALA20 (hydrophobic)	TYR28
GLY30	VAL44 (hydrophobic)
GLY31	
ASN32	
CYS33	
LYS34 (positively charged)	
GLY35	
MET36 (hydrophobic)	
THR37	
ARG38 (positively charged)	
THR39	
CYS40	
LEU43 (hydrophobic)	
CYS46	

Table 1

Figure Legends

Figure 1 – Structure of mung bean defensin VrD1 showing the secondary structure and disulphide bonds.

Figure 2 – Time sequence of the adsorption of VrD1 in orientation 1. Positions of charged amino acid residues (ARG1, LYS12, LYS34) that play a role in initial docking and anchoring of the defensin at the bilayer interface are shown for conformations a-f.

Figure 3 – Time sequence of the adsorption of VrD1 in orientation 2. Positions of charged amino acid residues (LYS7, ARG26, ARG38) that play a role in initial docking and anchoring of the defensin at the bilayer interface are shown for conformations a-f.

Figure 4 – Minimum distance of residues in VrD1 to DPPC bilayer averaged over the last 40ns of the simulation. The N-terminal is residue 1.

Figure 5 – (a) Van der Waals energy between VrD1 and DPPC bilayer; (b) Coulomb energy between VrD1 and DPPC bilayer.

Figure 6 – Secondary structure assignment for VrD1 defensin adsorbed in orientation 1 and 2 determined using DSSP (Direct Secondary Structure Prediction) (Kabsch & Sander, 1983). The main secondary structure features (β-sheets and α-helix) are stable and undisrupted throughout the simulation in both orientations.

Figure 7 - Root mean square deviation (RMSD) of the backbone atoms of the defensin chains.

Figure 8 – Radius of gyration of the defensin molecules over the course of the simulations. The overall radius of gyration (R_{gtotal}), and the x, y and z components (R_{gx}, R_{gy} and R_{gz}).

Figure 9 – Eccentricity of the shape of the adsorbed VrD1 protein over the simulation run. The horizontal solid line represents the average eccentricity of the native, non-adsorbed VrD1 molecule simulated in a water box. The two broken horizontal lines show ± standard deviation of the mean eccentricity of the native conformation.

Figure 10 – Order parameter for the acyl chains in the DPPC bilayer.

Figure 1

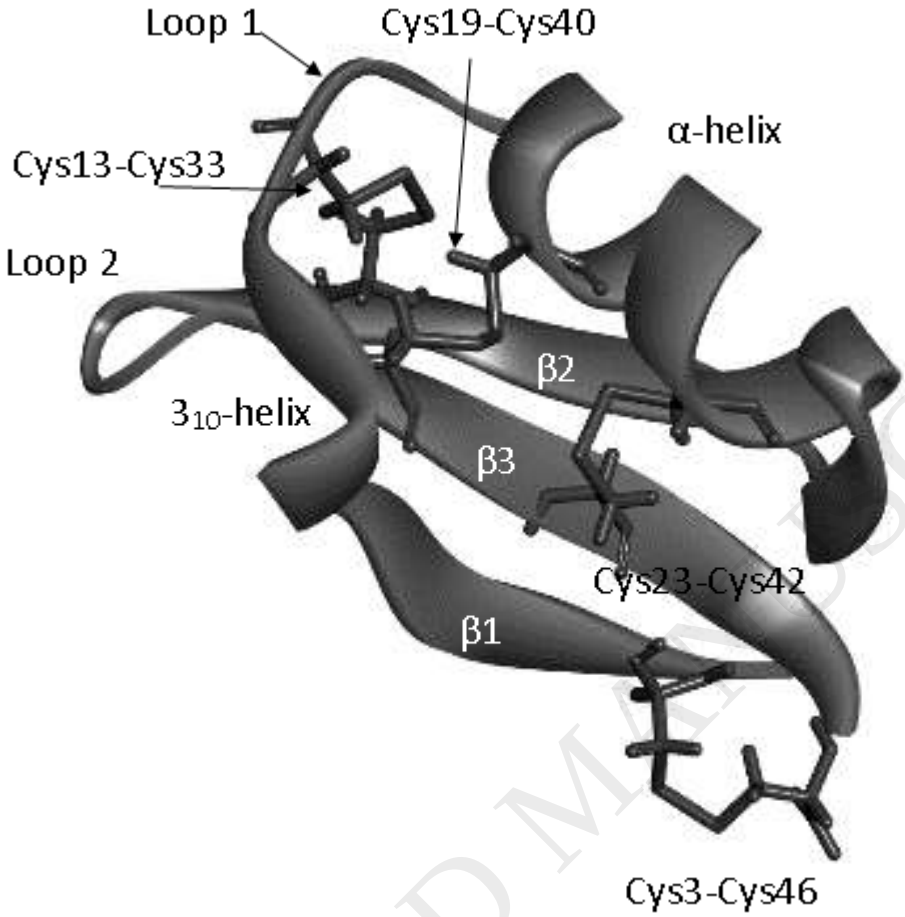

Figure 2

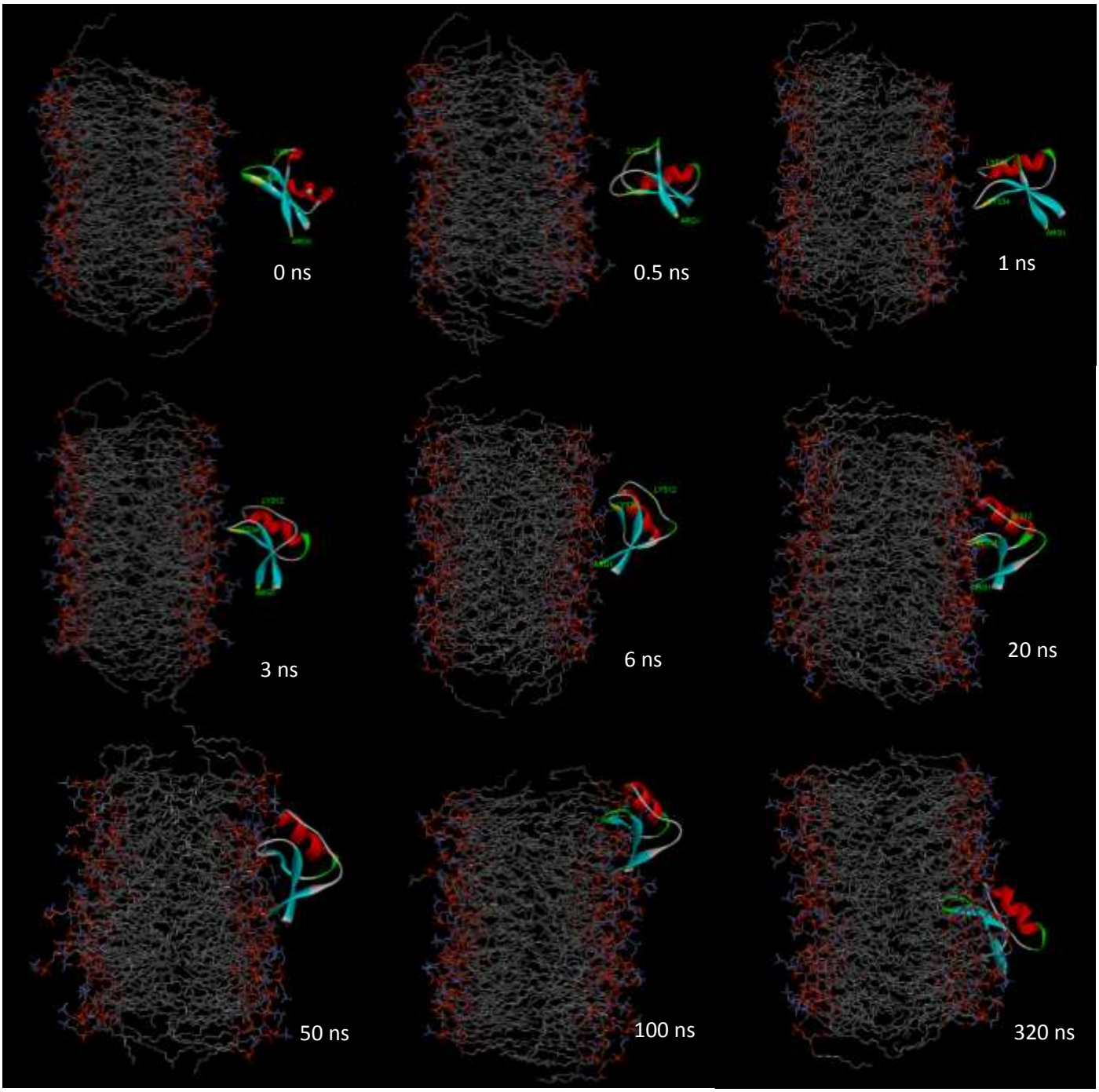

Figure 3

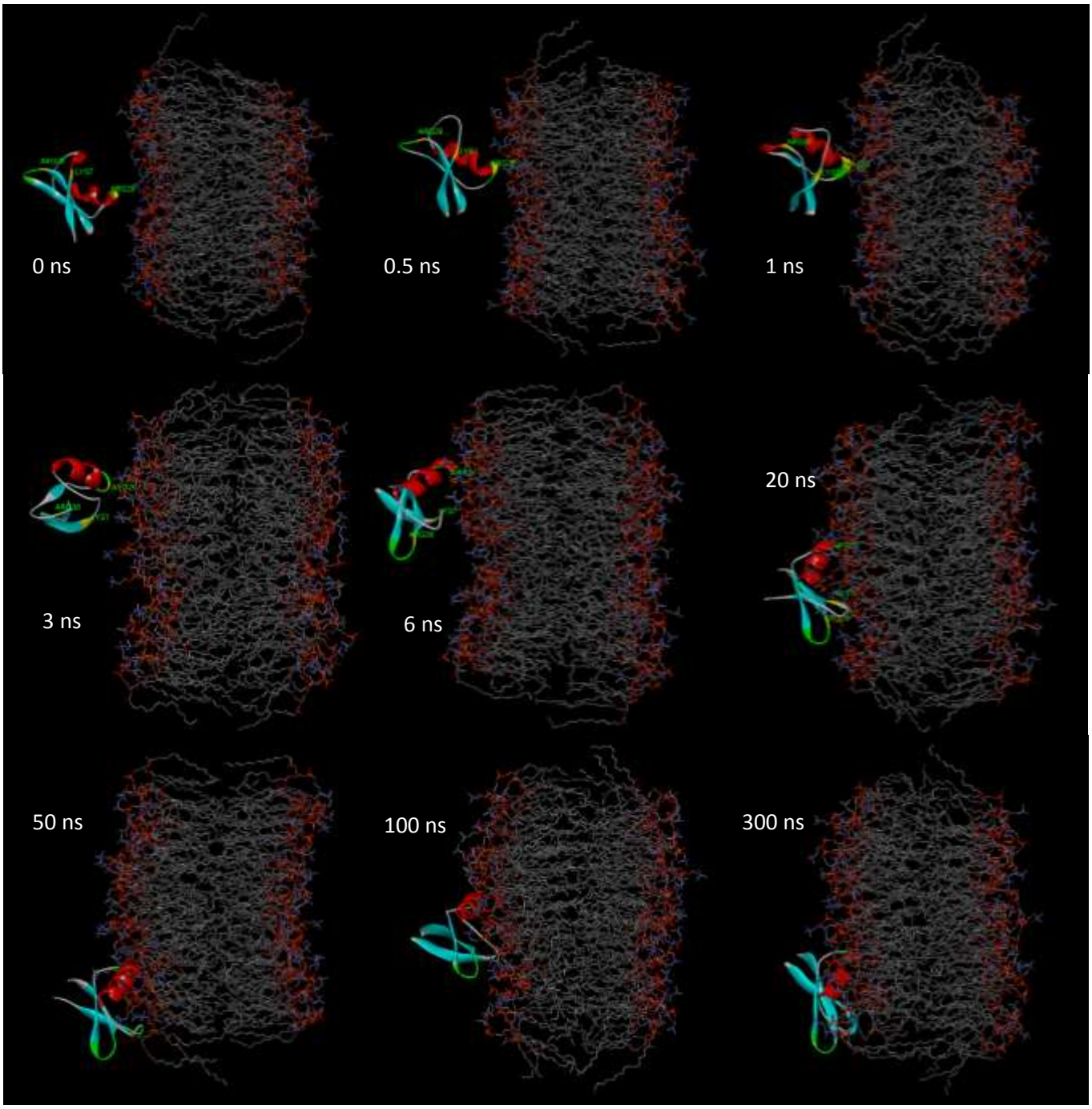

Figure 4

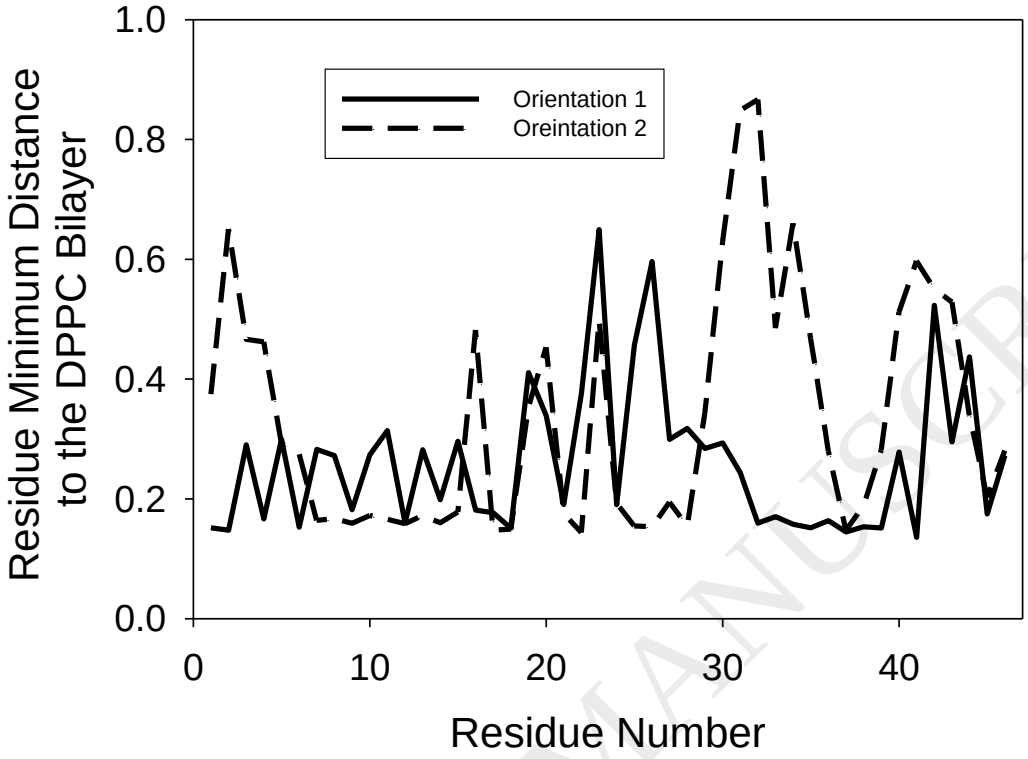

Figure 5

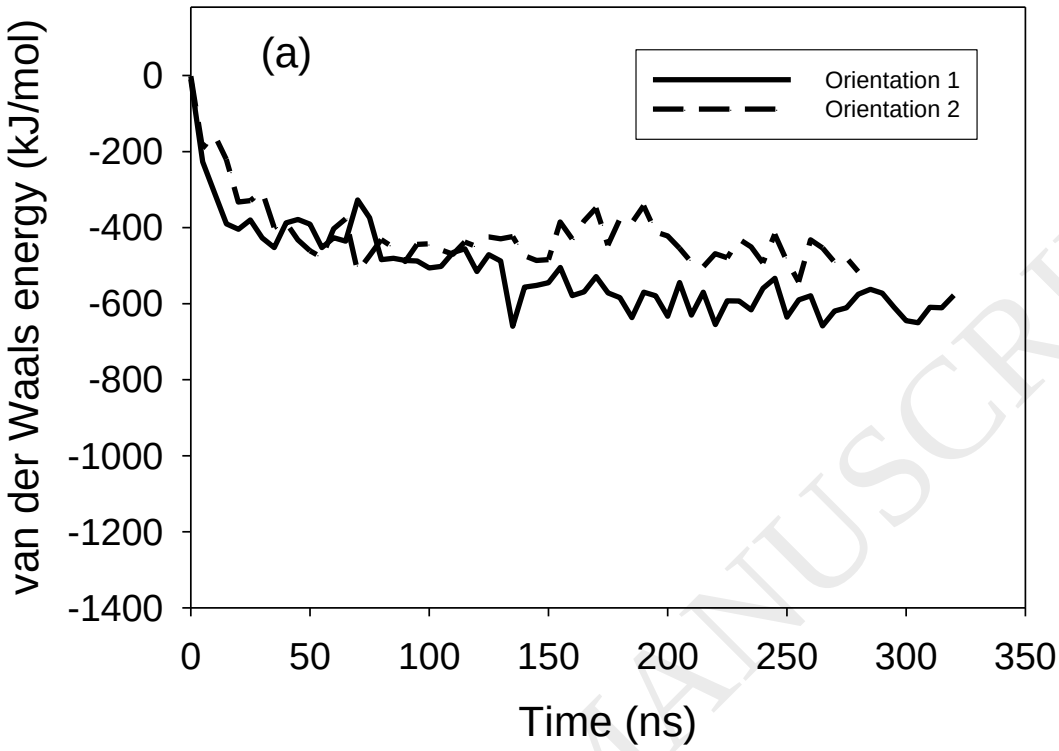

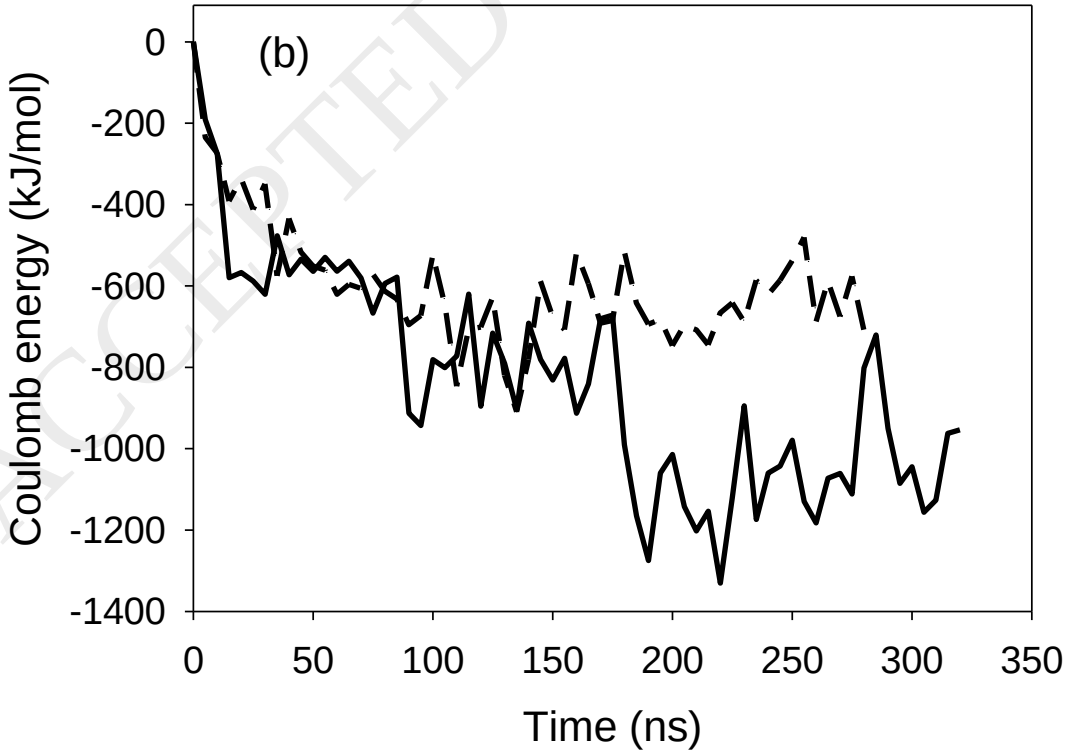

Figure 6

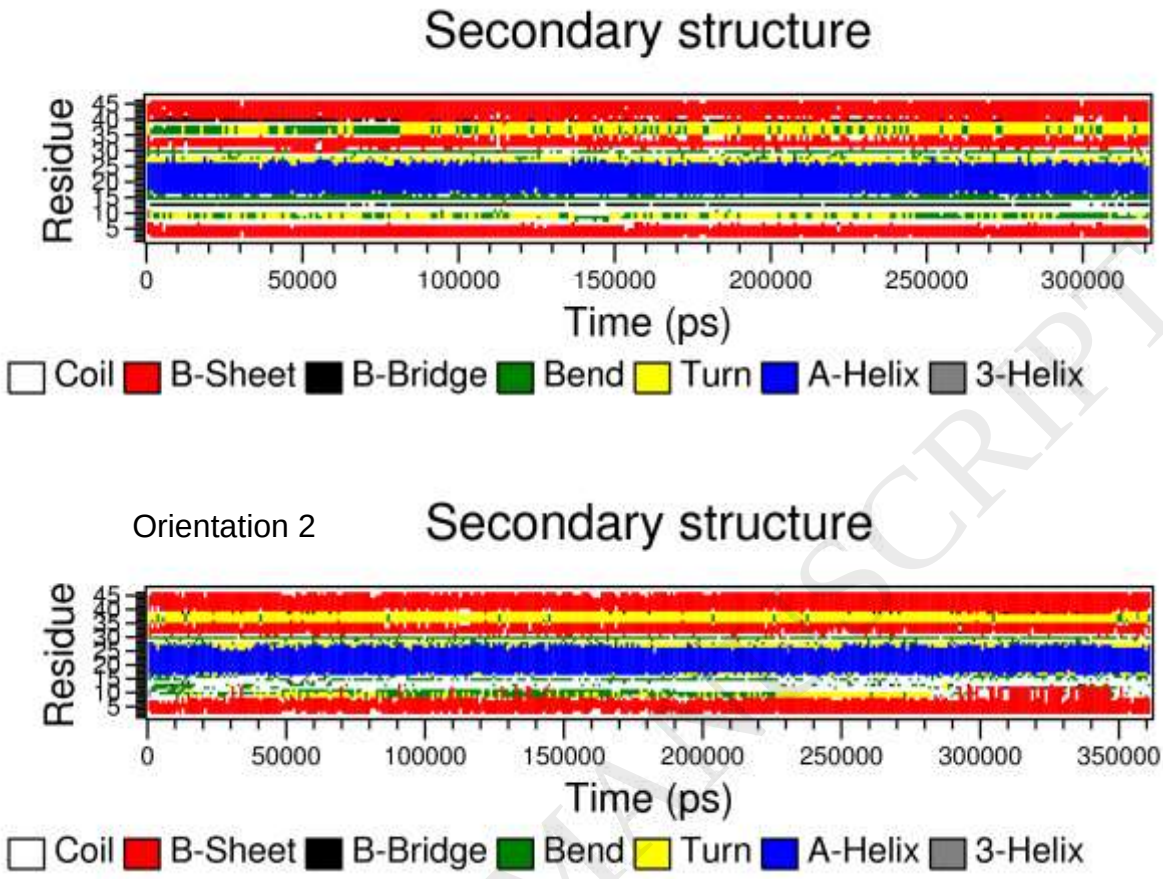

Orientation 2

Figure 7

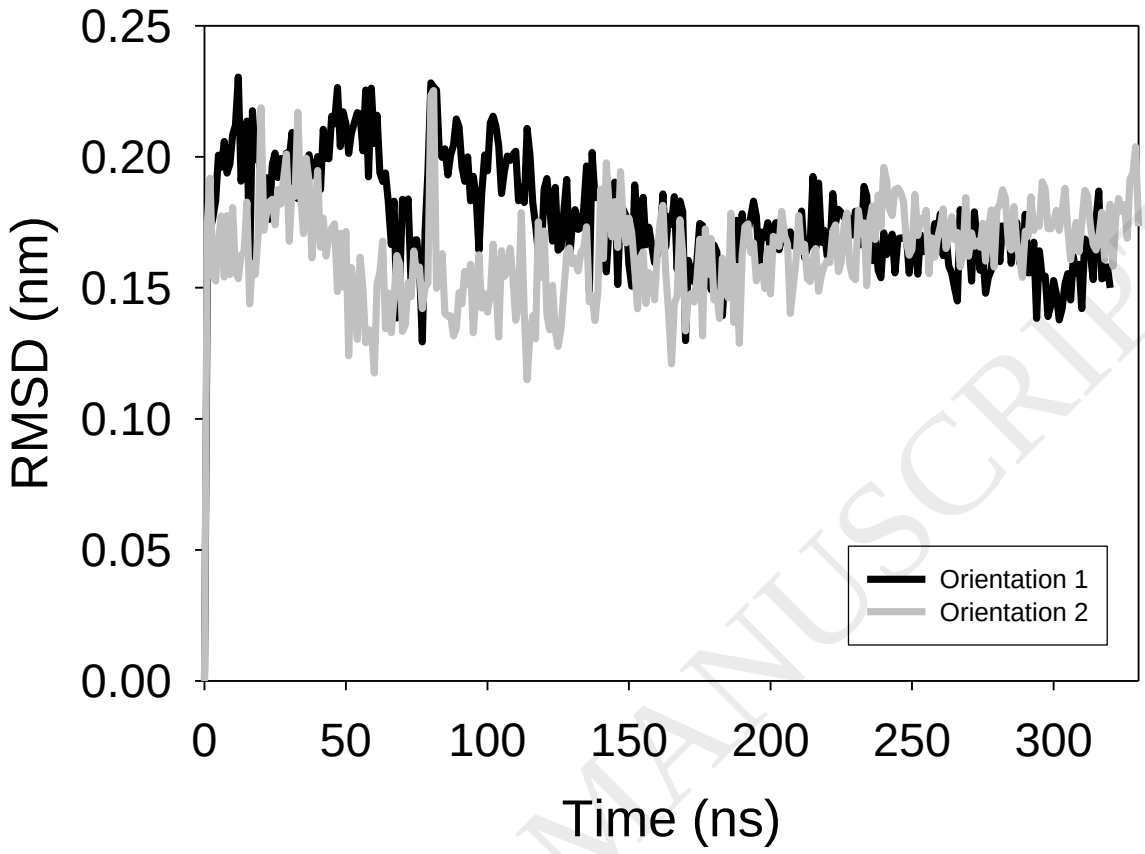

Figure 8

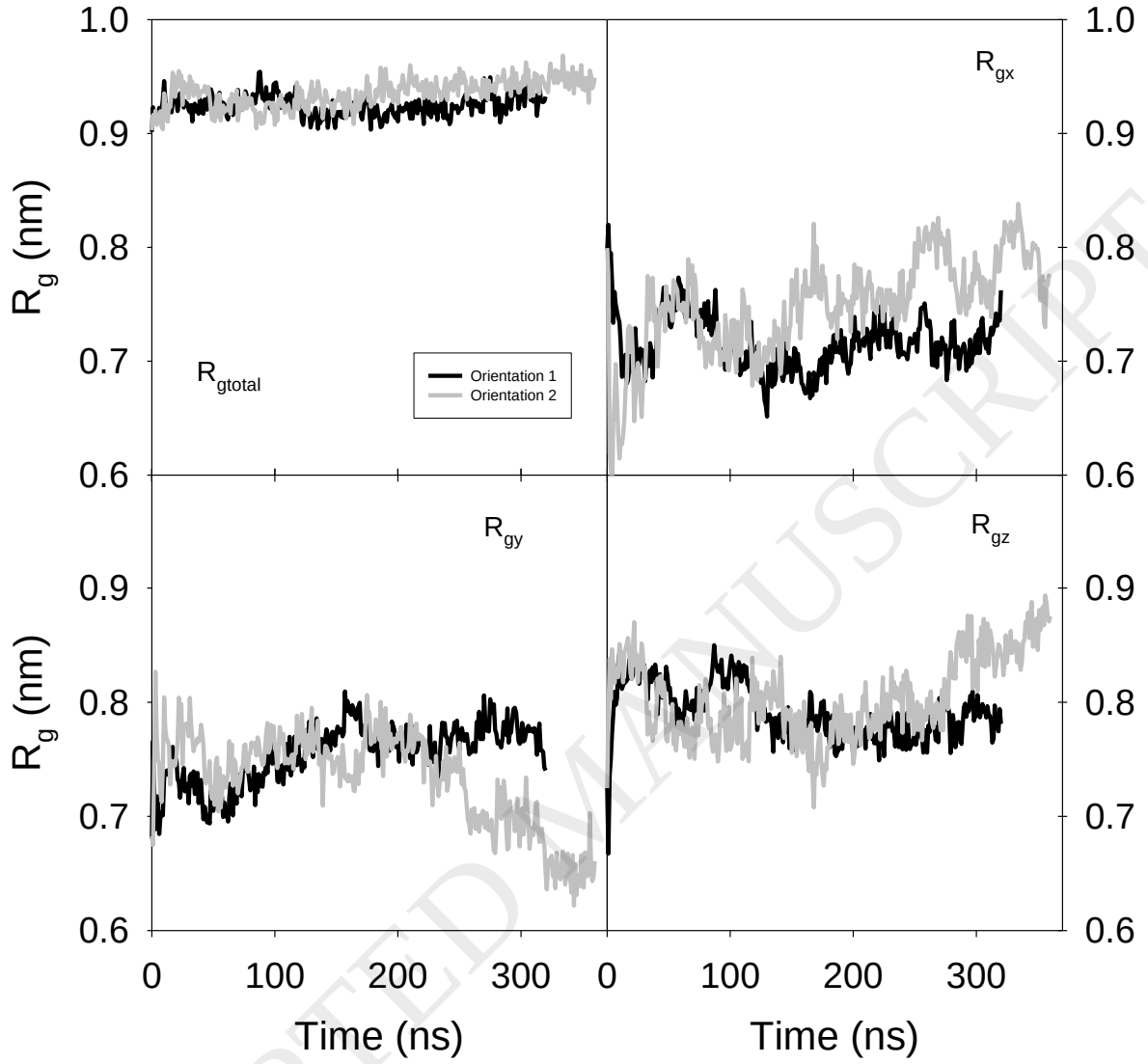

Figure 9

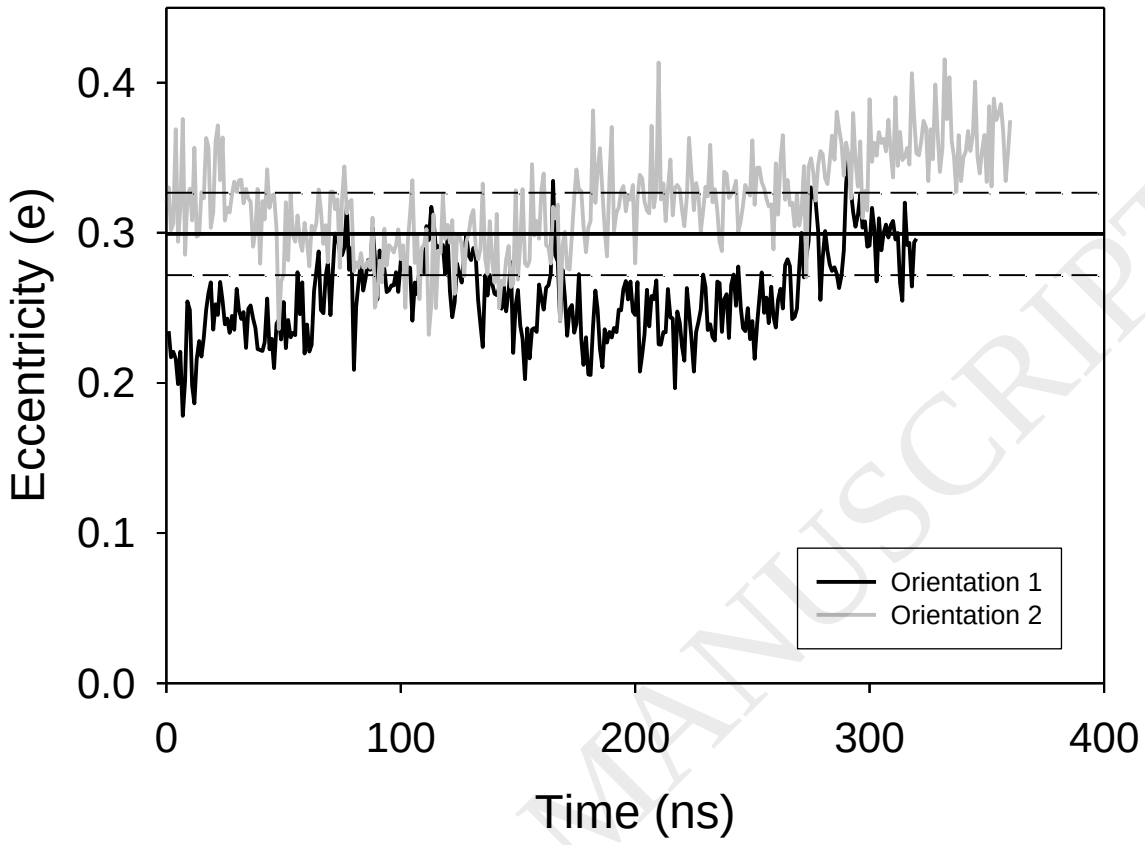

Figure 10